



Fabrication of 3D Microfluidic Channels and In-Channel Features Using 3D Printed, Water-Soluble Sacrificial Mold

Wei Huang Goh and Michinao Hashimoto*

Recent advent of additive manufacturing potentiates the fabrication of microchannels, albeit with limitations in resolution of printed structures, freedom of geometry, and choice of printable materials. Herein, a method is developed by sacrificial molding to fabricate microchannels in various polymer matrices and geometries. This method allows for rapid fabrication of 3D microchannels and channels harboring intricate in-channel features. The method uses commercially available fused deposition modeling 3D printer and filament made of polyvinyl alcohol (PVA). Mechanically stable molds are fabricated for 3D microchannels that can be completely removed in water. Importantly, the PVA mold is stable and resilient in hydrogels despite being hygroscopic. Perfusion channels are fabricated in biocompatible substrates such as gelatin and poly(ethylene glycol) diacrylate. Fabrication of the network of 3D multi-layer microchannels is demonstrated by preassembling sacrificial molds from modular pieces of molds. Intricate staggered-herringbones grooves (SHGs) are also fabricated within microchannels to produce micromixers. The versatility and resilience of the method developed here is advantageous for biological and chemical applications that require 3D configurations of microchannels in various matrices, which would not be compatible with fabrication by direct 3D printing and softlithography.

1. Introduction

This paper describes methods to fabricate 2D and 3D microchannels using water-soluble sacrificial molds fabricated by fused deposition modeling (FDM) 3D printer. The method we developed permits to fabricate truly 3D channels—the network of microchannels with 3D interconnections, and the microchannels with intricate 3D features within microchannel unlike monolithic channels fabricated via photolithography. We validated seven different materials—polymer resins and hydrogels—for their suitability to fabricate microchannels by this method. Microfluidics is a technology that encompasses manipulating or processing fluids in a channel at the micro-scale. It offers advantages in terms of the small sample volume and the small size scale of required platform.^[1] Over the last decade, the advent of microfluidic technologies has spurred

the development of specialized tools to facilitate chemical, optical, and biological analysis.^[2,3] To date, the application of microfluidics has evolved from generation of tailored emulsions,^[4] point-of-care diagnostics devices,^[5] analytical reaction-ware,^[6] and organs-on-chip devices for biomedical assays.^[7]

Fabrication of microfluidic devices has evolved from 2D processes such as etching and photolithography, which are typically performed under cleanroom conditions. A well-established process, soft-lithography,^[8] allows for the fabrication of microchannels using a mold of SU-8 patterned on a silicon wafer.^[9] This process is the most suitable to fabricate 2D (or monolithic) devices. The fabrication of 3D geometries within these microchannels would require layer-by-layer process and deliberate alignment,^[10,11] and the process is time consuming and unpractical for researchers without appropriate experiences.^[12] Recent advances in additive manufacturing technologies have paved a way to fabricate microfluidic devices

with 3D design of channels.^[13] Examples of additive manufacturing include selective laser sintering,^[14] stereolithography (SLA),^[1] laminated object manufacturing,^[10] inkjet printing of photopolymer,^[15] and fused deposition modeling.^[6,16] Generally, these additive manufacturing technologies require a 3D computer-aided design (CAD) model of interest transformed into a computer code describing the model sliced in layers. The codes are used to print the 3D object layer-by-layer in vertical dimension. At present, the entire microfluidic channel has been fabricated by SLA,^[1] polymer jetting,^[15] and FDM.^[6] 3D printing has exhibited prospects to be methods for fabrication of microchannels alternative to softlithography. Potential drawbacks of 3D printing are surface roughness,^[1,15] optical clarity,^[6] biocompatibility,^[15] and selection of materials available for printing.^[6,15]

Alternatively, microchannels can be fabricated by removing microscale structures embedded in matrix of choice. This process is known as sacrificial molding.^[17–23] Sacrificial molding is a rapid prototyping and affordable approach to produce microchannels harboring 3D design. Molds are microfabricated, embedded in a matrix, and subsequently removed to leave the empty space for microchannels. To this end, researchers have used controlled extruders to create sacrificial molds. For example, sugar glass strands^[21] and shellac microfibers^[24] extruded by cotton candy machine were used to create perfusable

W. H. Goh, Prof. M. Hashimoto
Pillar of Engineering Product Development
Singapore University of Technology and Design
8 Somapah Road, Singapore 487832, Singapore
E-mail: hashimoto@sutd.edu.sg

The ORCID identification number(s) for the author(s) of this article can be found under <https://doi.org/10.1002/mame.201700484>.

DOI: 10.1002/mame.201700484

3D mesh network in polydimethylsiloxane (PDMS) and transglutaminase enzymatically crosslinked gelatin (TG gelatin), respectively. The sugar-based substrate was removed in water and shellac substrate was removed in an ammonium solution. Similarly, poly-*N*-isopropylacrylamide (PNIPAM) fibers were melt spun by a custom-made extruder to produce perfusion networks to support mass transportation of medium to sustain tissue growth.^[25] PNIPAM mesh was removed by soaking in culture medium. Devices fabricated by these methods have limited geometry and uncontrolled dimensions, which can possibly confound perfusion rate or volume of fluids through the device. Alternatively, sacrificial molds with controlled dimension can be fabricated with a digitally controlled liquid dispenser or filament extruder. Aqueous and organic ink,^[23,26] carbohydrate-based substrates,^[20,21] eutectic metal,^[27] acrylonitrile butadienestyrene,^[28] and hydrogels (agarose and gelatin)^[19,22] are demonstrated as materials for sacrificial molds to create microfluidic channels.

Despite vast potentials of sacrificial molding to create various microchannels, the method has not been fully utilized. Currently demonstrated methods of sacrificial molding rely on either custom-made instruments to pattern molds,^[20,29] postprocessing to enhance the stability of molds,^[20,21,29] or organic solvents to remove molds.^[24,28] Moreover, structures of sacrificial molds made of liquids or gels are difficult to sustain without support materials, and layer-by-layer casting of matrix is required to fabricate 3D channels.^[20,23] Polyvinyl alcohol (PVA) is a water soluble thermoplastic and it is widely used as a support material for FDM 3D printing.^[30] PVA has been used to create porous scaffolds in PDMS.^[18] Because it is hygroscopic; however, a water resistant coating is typically required when it is used as sacrificial material to produce perfusion channels in hydrogels.^[17,31]

Herein, we demonstrated the use of PVA molds patterned by an FDM 3D printer for fabrication of microchannels with simple (2D, monolithic) and complex (3D, non-planar) geometries. Intricate features within microfluidic channels are still difficult to fabricate via softlithography and yet to be demonstrated to fabricate by sacrificial molding. We selected PVA as a sacrificial material so that the removal of the material can be fully completed in an aqueous environment. We presented FDM as an affordable tool for fabrication of microchannels on the order of 200 μm in width and 100 μm in height and demonstrated that our approach is compatible with wide range of polymeric matrixes.

Our work has highlighted some of the useful features of sacrificial molding for fabrication of microchannels. First, the entire fabrication can be completed using a commercially available FDM 3D printer and filament.

Second, the process is completed only using aqueous solutions, without protective coatings of the molds even when used with hydrogels. In addition, we demonstrated that this method offered wide freedom of design of microchannels, conferred by CAD, digital fabrication, and preassembly of sacrificial molds. The method we developed here should benefit a wide range of researchers by providing a simple route to fabricate microfluidic channels with minimum requirement of fabrication tools.

2. Results and Discussion

2.1. Fabrication of Microfluidic Channels by Sacrificial Molding

The process to fabricate a microfluidic device by sacrificial molding using 3D printed PVA mold is illustrated in five steps (Figure 1). A computer-aided-design (CAD) of desired mold was developed and subsequently processed using software to create G-codes. The G-codes are scripts interpreted by the 3D printer to extrude filament in horizontal (x , y) and vertical (z) dimensions

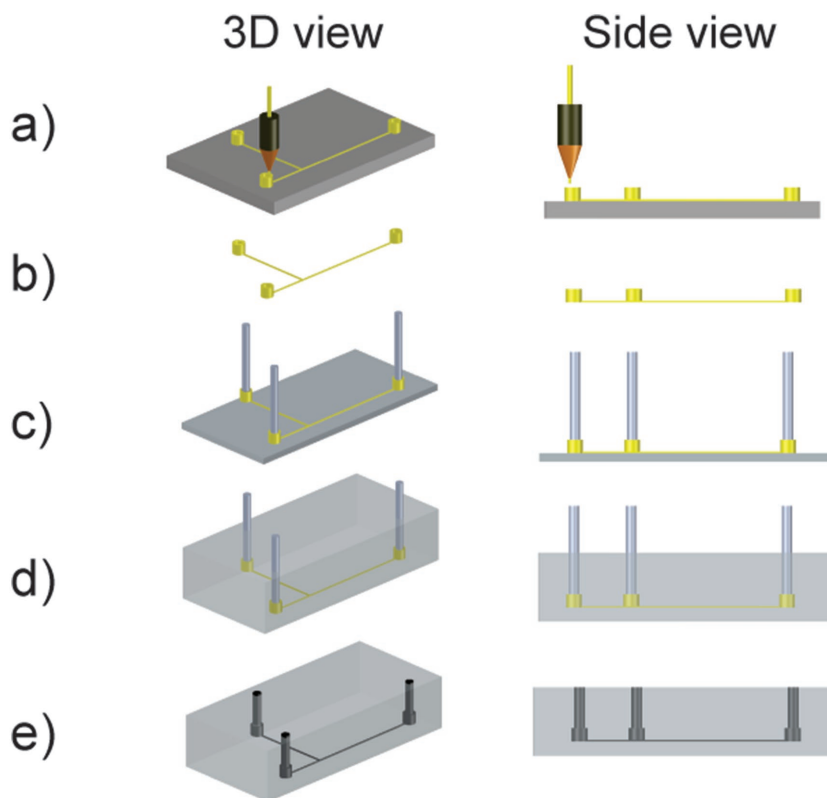


Figure 1. Schematics describing the steps of sacrificial molding to fabricate microfluidic channels in castable matrices. 3D view and side view of the processes are illustrated. a) A sacrificial mold is patterned with a PVA filament using an FDM 3D printer. b) A completed sacrificial mold is removed from the printing bed. The mold has the patterns of microchannels and sockets for PTFE tubes that serves as inlets and outlets. c) Short segments of PTFE tube (10 mm) are attached to the sockets patterned on the mold. The mold is placed on a thin layer of the cured polymer matrix. d) Fully degassed, uncured polymer is casted to embed entire PVA mold and including the inlet/outlet sockets that were connected to PTFE tubes (leaving about 5 mm segment of PTFE tube protruding from the matrix to facilitate exposure of PVA later). e) The PVA mold is exposed to water in an ultrasonic water bath. Intact microfluidic channels were revealed after removing the PVA mold.

(Figure 1a,b). It took less than 2 min to complete the printing of T-junction geometry and three inlets/outlets (nominal dimension; length of long channel was 30 mm, length of short channel was 15 mm, and the height and width of entire channel was 200 μm). In addition, it took less than 14 min to complete the printing of the mold with intricate features like the herringbone patterns (Figure 5, dimension; nominal length of channel was 70 mm, width was 1.2 mm, and total height of structure was 1 mm).

Since PVA is hygroscopic, it was necessary to avoid exposing printed molds to moisture. We observed that the printed molds with the width of 200 μm turned flaccid after 5 min of exposure to ambient air. Printed molds with the width of 1 mm and above turned flaccid after overnight exposure to ambient air. To maintain the quality and structural integrity of PVA, both PVA filaments and printed molds were stored in an airtight container filled with silica beads. A strip of PVA filament (≈ 100 cm) was prebaked in the oven overnight and kept in a dry box before usage. Similarly, the mold was removed from the print bed after printing and transferred to a dry box immediately to minimize exposure to moisture. Thereafter, printed molds (Figure 1b) were used for molding. The printed molds were designed with small holes ($d = 0.8$ mm) where a short (1 cm) segment of polytetrafluoroethylene (PTFE) tube was inserted. These segments of PTFE tube preserved the inlet and outlet holes in the cured polymer matrix.

In order to embed a PVA mold completely, a thin layer of matrix of interest was used as a base (Figure 1c). The preexisting base layer ensured to enclose the sacrificial molds in the matrix. Matrix of interest was added to submerge the entire mold and then fully cured (Figure 1d). Thereafter, the PTFE tube was removed to expose the PVA mold to water. The matrix together with the embedded mold was subjected to ultrasonication to accelerate dissolution of PVA in deionized water. The efficiency of ultrasonication to improve the rate of dissolution has been studied in ref.^[32] In our study, a T-junction mold (200 μm width, 200 μm height, and 1.5 mm length) was removed after 3 h and complicated mold such as a chaotic mixer with staggered herringbone structures (1200 μm width, 1000 μm height, and 70 mm length) took 36 h, to create the void space defined by the mold. Fabrication of microchannels using water-soluble, 3D printed molds offers freedom of design ranging from simple T-junctions to complex channels such as chaotic mixers. The time required to complete the fabrication depends on the dimension and design of the mold, as the evacuation of the mold in water would be the most time-consuming step.

2.2. Characterization of Microfluidic Channels after Removal of PVA Mold

To study the minimum dimension of the channels that can be fabricated by our

methods, we varied two parameters pertinent to the FDM printer: nozzle diameter (d) and layer heights (h). The smallest features were obtained when $d = 200$ μm and $h = 100$ μm reproducibly. We used multiples of 200 μm for the horizontal dimensions (x, y), and multiples of 100 μm for the vertical dimension (z) in the design of the molds. To determine the fidelity of the replication of the mold, we characterized nominal dimensions of channel height and the resulting height (Figure 2a), and nominal width of channel and the resulting width (Figure 2b) after removal of embedded mold in PDMS. The mean height obtained were 117 μm for 100 μm (SD = 17 μm), 210 μm for 200 μm (SD = 25 μm), 283 μm for 300 μm (SD = 13 μm), and 413 μm for 400 μm (SD = 32 μm). The mean width was 232 μm (SD = 25 μm), 427 μm (SD = 16 μm), and 652 μm (SD = 41 μm) for the nominal width of 200, 400, and 600 μm respectively. The deviation in width we obtained is smaller compared to 67.8 μm reported by a characterization test performed on parts printed by an FDM 3D printer.^[15] Optical image depicting cross-section of microchannel after removal of mold showed morphology of the removed mold (Figure 2c). The imprint that resembled the sequential stacking of layers of material was evident at channel height of 200 μm and greater. These patterns are inherent to the mechanism of printing in the FDM printer.

The scope of this study is to discuss fabrication of micro-scale structures, and the maximum dimension of the channels was not explored. In principle, it is possible to create millimeter to centimeter scale channels and cavities using sacrificial molding, while the time required to remove the PVA mold would increase as the size of the mold increases. The time required to dissolve PVA molds would depend on multiple

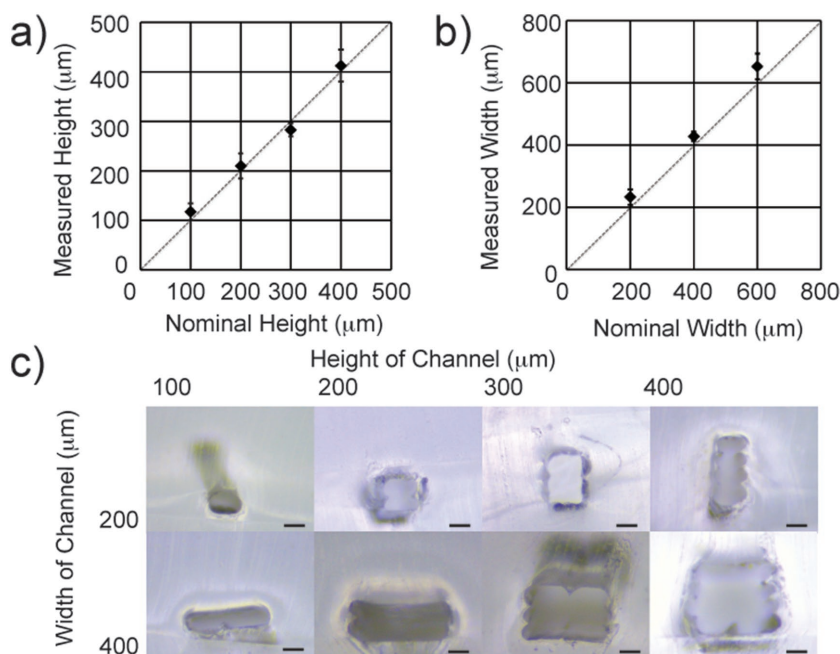


Figure 2. Characterization of the width and height of microchannels fabricated using 3D printed, PVA molds. a) Characterization of height of fabricated microchannels with respect to the variation of nominal height in CAD. b) Characterization of width of fabricated microchannels with respect to the variation of nominal width in CAD. c) Images of cross-sections of microchannels obtained after removal of PVA mold. The data are mean \pm SD ($n = 20$ for (a) and $n = 12$ –40 for (b)) (Scale bar = 100 μm).

factors, such as the area exposed to aqueous media, the size of mold, and the infill patterns of the mold determined by the mode of FDM printing.

2.3. PVA as a Material for Sacrificial Molding

We demonstrated that a T-junction mold at the nominal dimension of 200 μm height and 200 μm width was stable in seven substrates we tested (rigid polymers, soft polymers, and hydrogels) during casting and removal of the mold. The T-junction geometry was replicated in heat curable hard polymers such as rigid polyurethane (PU) and epoxy (Figure 3a,b) and heat curable soft polymers like flexible polyurethane and PDMS (Figure 3d,e). The T-junction geometry was also reproduced in ultraviolet (UV) light curable hard polymers and hydrogel like Norland Optical Adhesive 81 (NOA 81) and poly(ethylene glycol) diacrylate (PEGDA), respectively (Figure 3c,g). Remarkably, Figure 3f,g shows that the channel was also faithfully fabricated in heat and UV curable hydrogels (gelatin and PEGDA). Based on our observations, a PVA mold in the order of 200 μm width and height was stable during casting and for the duration of time that hydrogel matrices cured (10 s). We note that viscous matrixes like the polyurethane and PDMS did not affect the integrity (i.e., shapes and dimensions) of the PVA mold.

When performing sacrificial molding, materials for the mold and for the matrix must be carefully selected. We highlight two processes where compatibility of materials is essential: (1) casting matrix to embed the mold and (2) removing the mold from the cured matrix. Casting of molds may affect integrity of mold. Intricate features are most vulnerable to chemical or mechanical damages, and damages to the mold are reflected

on features replicated after removal of mold. Removing of molds may adversely affect the physical nature of matrix, as the mold and substrates are exposed to a solvent to remove the mold. Water used as a solvent allowed to preserve the nature of the matrices while dissolving the embedded mold.

2.4. Versatile Compatibility with Polymers and Hydrogels

For sacrificial molding to appeal to a wide range of application, an appropriate choice of solvents to dissolve molds is critical. Visual inspection under an optical microscope showed that the embedded PVA mold was successfully removed within the seven matrixes tested in this report (Figure 3). During the removal of the mold, the entire structure (i.e., matrix containing mold) was submerged in the solvent. Under this circumstance, the integrity of the matrix during exposure to the solvent must be preserved.

We consider successful fabrication of microchannel when three criteria were met: (1) full dissolution of PVA mold in matrix to reveal microchannel, (2) no detectable seepage into the matrix, and (3) no disintegration of matrix or collapse of the microchannel. The perfusion of red dye solution into microchannels in each substrate suggested that fabricated microchannels were intact and the matrixes cured successfully (Figure 3a–g). We note that it is possible that PVA molecules adsorb and remain on the surface of the microchannels after they are removed macroscopically,^[33] which could render the surface of the channel hydrophilic.

Fabrication of microchannels using materials alternative to PDMS can be beneficial for intended applications.^[34] Chemical resistant PU and epoxy are widely used as a matrix in microfluidics system, and they demonstrated successful application in

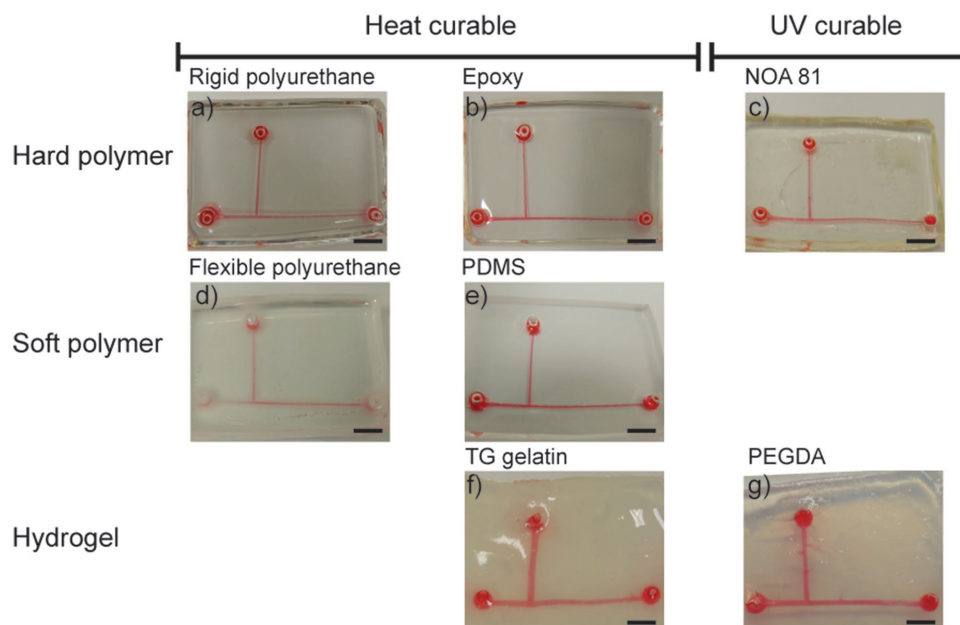


Figure 3. Optical images of microchannels perfused with aqueous solution of red dye in seven different polymer matrices. a) Rigid polyurethane. b) Epoxy. c) NOA 81. d) Flexible polyurethane. e) PDMS. f) TG gelatin. g) PEGDA. This method of fabrication is applicable to rigid and soft polymer matrices, which are cured either by heat (i.e., elevated temperature) or exposure to UV light. The length of horizontal and vertical channels is 30 and 15 mm, respectively. Both the width and height of the channels are 200 μm (Scale bar = 5.0 mm).

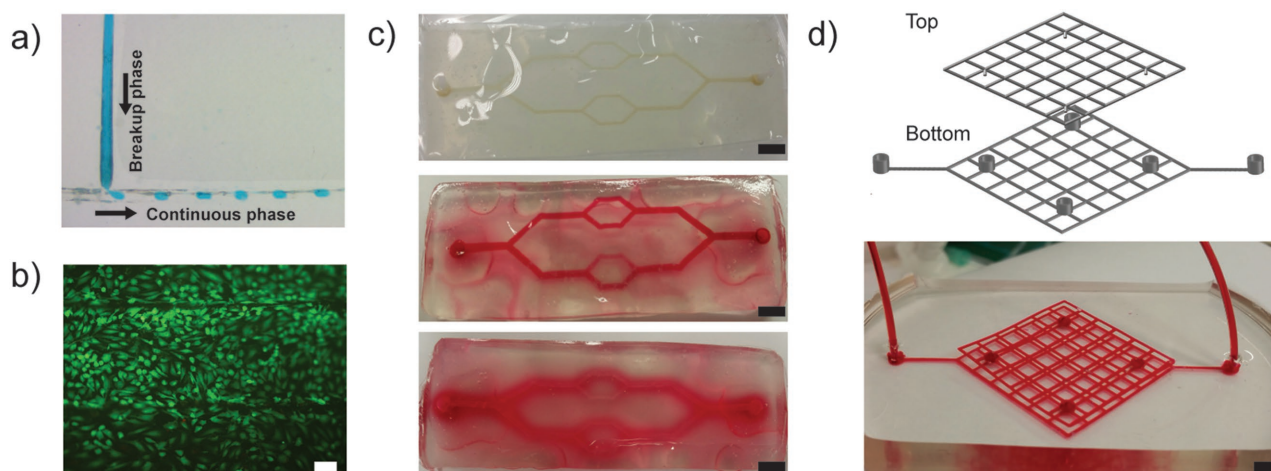


Figure 4. Optical images showing designs and applications of microchannels fabricated using sacrificial molding. a) Multiphase flows and droplet generation. Blue colored water ($5 \mu\text{L min}^{-1}$) was used as the dispersed phase, and 3% Span 80 in hexadecane ($15 \mu\text{L min}^{-1}$) was used as the continuous phase to produce water droplets in an oil phase. b) Flow culture of cells. Live/dead florescence stain of HUVECs cultured in the PDMS microchannel is shown. c) PVA mold was embedded in TG gelatin (top), microchannels was perfused with solution of red dye after removal of PVA mold (middle), and diffusion of the red dye into the matrix of the gelatin after 24 h. d) Schematics of 3D microchannels arranged in interlocking grid design with male and female connectors are illustrated (top) and the channels are perfused with a solution of red dye after removal of the assembled mold (bottom). Channel width (w) and height (h), denoted as (w, h), was a) ($200 \mu\text{m}, 200 \mu\text{m}$), b) ($1200 \mu\text{m}, 400 \mu\text{m}$), c) ($600 \mu\text{m}, 400 \mu\text{m}$) for main branches, and ($400 \mu\text{m}, 400 \mu\text{m}$) for sub branches), and d) ($400 \mu\text{m}, 400 \mu\text{m}$), respectively (Scale bar = $100 \mu\text{m}$ for (b), 7 mm for (c), and 2 mm for (d)).

the chemical,^[2] biological,^[35] and biomedical field.^[36,37] Alternatively, the UV curable thiolene-based matrix, NOA 81, was seen as a popular substitute matrix capable of withstanding exposure to organic solvents^[38,39] and have similar optical clarity as PDMS but not permeable to air or moisture.^[40] Furthermore, surface modifications performed on NOA 81 were more stable than PDMS.^[38] In this study, NOA 81 was used straight from the bottle, no degassing or mixing of polymer was required, and curing was completed within 10 s. Channels made of these materials are potentially useful for chemical and biological reactions that would not be performed in PDMS channels due to its chemical compatibility.

Bioinspired applications may need to rely on biomimetic matrixes, which confers physiologically similar texture and hardness to sustain growth on the bench. These applications typically require less stringent requirement with resolution but prefer inclusion of hydrodynamics and 3D arrangement of cell-laden structures to mimic in vivo conditions. The biocompatibility of PEGDA and TG gelatin were previous demonstrated.^[41–43] Our results may complement approaches in tissue engineering used to fabricate microchannels for perfusing fluids through tissue construct currently in practice.^[25,44]

2.5. Applications of Microfluidic Channels Created by Sacrificial Molding

To demonstrate that microchannels fabricated by sacrificial molding can be used for typical applications in microfluidics, we tested the T-junction microfluidic channel in PDMS for droplet generation. A dispersed phase of blue colored water was infused from the vertical channel and a continuous flow of 3% Span 80 in hexadecane was infused from the horizontal channel to generate water in oil (W/O) droplet (Figure 4a). A

straight microchannel in PDMS was tested for flow culture of Human Umbilical Vein Endothelial Cells (HUVECs). Live/dead fluorescence stain of HUVECs seeded on the surface of the microchannel coated with 0.2% gelatin showed that cells were viable when assayed on day 2 postseeding of the device (Figure 4b).

We detected several focal planes in the observation using phase contrast microscopy, which indicated the presence of uneven surface in the channel. It is plausible that the uneven surface was produced by inherent pattern of the PVA sacrificial mold. In this work, we used an FDM 3D printer to pattern extruded PVA in the dimension of $200 \mu\text{m}$ in the x and y direction and $100 \mu\text{m}$ in the z -direction. When the mold was greater than $200 \mu\text{m}$ in width and $100 \mu\text{m}$ in height, grooves formed between the adjacent extrusions. The grooves were filled with matrix materials, and formed “hump” like patterns on the inner surface of the microchannels. Optical images (Figure 2c) depicted the hump-like patterns in the microchannels greater than the minimum dimensions. To avoid these uneven surfaces, postprocessing methods may be employed to improve the surface roughness of the FDM printed molds.^[45]

To study and demonstrate the stability of PVA mold casted with TG gelatin, we adopted the design of microchannel from a previous demonstration.^[17] The PVA mold with main and sub-branches were intact and swelling was not observed during gelation (Figure 4c, top). After the mold was removed, clear channels were revealed and an aqueous solution containing a red dye was perfused (Figure 4c, middle). The design retained in the hydrogel illustrates that, while PVA was hygroscopic,^[17] the integrity of the 3D printed mold was maintained in hydrogels when the enclosing matrix cured rapidly. We attributed this observation to the short time required for gelation ($\approx 10 \text{ s}$) for TG gelatin when the process was performed on an ice bath.

To confirm that the microchannel was successfully formed in TG gelatin, we filled the channel with an aqueous solution containing red dye, and the channel was left for 24 h. The red dye diffused into the matrix surrounding the microchannels (Figure 4c, bottom). This result is consistent with a study that looked at boosting viability in cell-laden hydrogels by enhancing rate of material transport through the incorporation of perfusion channels.^[19] We note that another study reported that the removal of PVA in gelatin-based device had negligible implication on cell viability.^[17] Sacrificial molding for fabrication of microchannels within biomimetic matrix could be potentially useful for applications in tissue engineering.^[20,42]

2.6. Fabrication of Modular 3D Microfluidics Channels

Multiple sacrificial molds can be assembled to create a mold for microchannels that has 3D interconnections. To perform postassembly of 3D printed molds, two or more molds with complementary connection can be fabricated separately. The complementary connectors were placed and snapped together before casting in a substrate. We demonstrated this approach by fabricating two pieces of molds with male connectors (OD = 0.8 mm) and female connectors (ID = 1.6 mm), respectively (Figure 4d, top). The OD of the male connectors and the ID of the female connectors were optimized to account for the precision of printing of the relatively small, protruding structures. These two pieces of molds were then snapped together,

and casted in PDMS for sacrificial molding. After the removal of the mold, an aqueous solution containing red dye was perfused (Figure 4d, bottom). This demonstration suggests that sacrificial molding can be readily extended to include modularity for fabrication of channels consisting with various arrangements of modules, as well as channels with 3D arrangement of modules.

2.7. Fabrication of Microchannel with Internal 3D Structures

To illustrate the capability of fabricating microchannels with intricate 3D structures, we designed a PVA mold that has staggered-herringbones grooves (SHGs) on the base and at top of the channel in PDMS (Figure 5a). In our design, 16 bones arranged in two sets of eight bones orientated asymmetrically constituted one mixing cycle (Figure 5a). A single device contained three mixing cycles. A representative picture of the embedded PVA mold, channels after removal of PVA, and channels with dye solution are shown (Figure 5b–d). We compared the mixing capabilities of three channels: a straight microchannel (Figure 5e), a microchannel with SHGs only at the bottom of the channel (Figure 5f), and a microchannel with SHGs at the top and bottom of the channel (Figure 5g). Two parallel streams of solutions with red and green dye were introduced at $150 \mu\text{L min}^{-1}$ into the inlets and observed at four locations along the microchannel: (1) just after the inlets, (2) after first mixing cycle, (3) after second mixing cycle, and (4) after third mixing cycle.

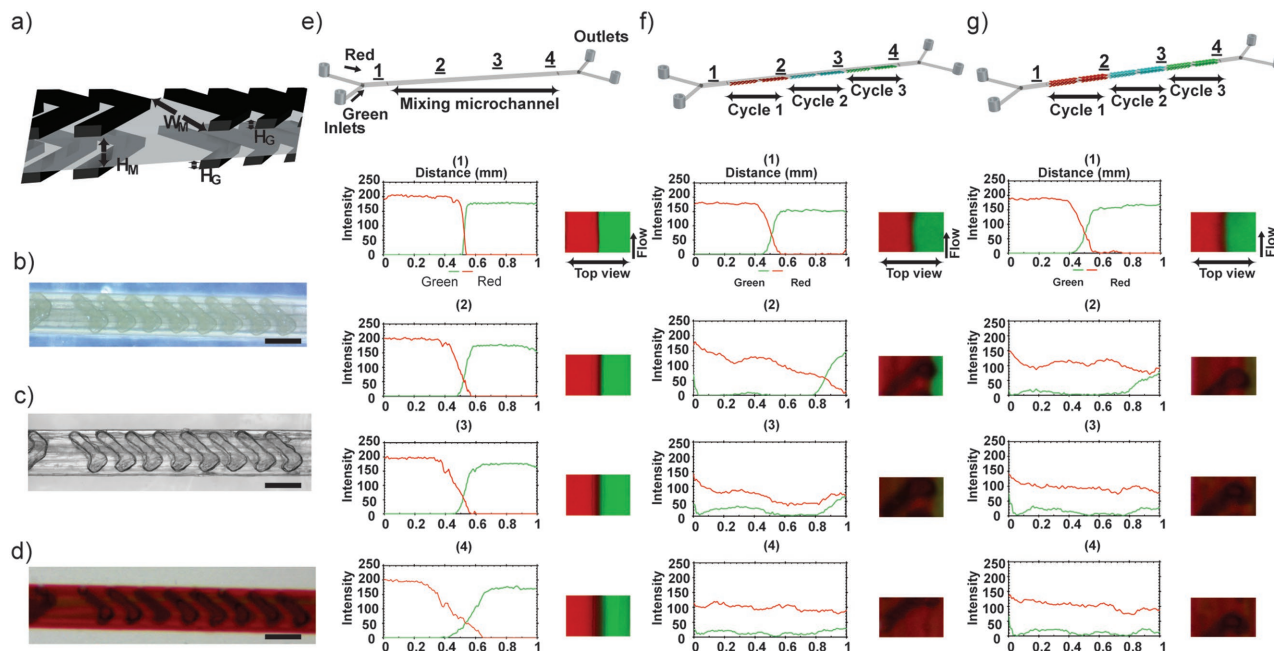


Figure 5. Device for chaotic mixing utilizing staggered herringbone grooves and corresponding mixing profile. a) 3D CAD design of PVA chaotic mixer with staggered herringbone grooves on the top and bottom of the microchannel. b) A image of top-down view of 3D printed PVA mold consisting staggered herringbone grooves on top of microchannel. These eight grooves also formed half of one mixing cycle. c) A image of 3D microchannel after removal of PVA mold. d) A image of solution of red and green dye mixed after flowing through device with staggered herringbone grooves. Mixing profiles of red and green dye solutions were analyzed from a top-down view taken at position 1, 2, 3, and 4. e) A straight microfluidic microchannel devoid of in-channel features as negative control, f) staggered herringbone on base of microchannel as positive control, and g) 3D microchannel with staggered herringbone grooves on the base and top of microchannel. The flow rates applied was $150 \mu\text{L min}^{-1}$. Width of microchannel (W_M) was 1.2 mm, height of microchannel (H_M) was 600 μm , and height of grooves (H_G) was 200 μm (Scale bar = 1 mm).

Mixing was caused only with diffusion in a simple channel (Figure 5e), while the addition of one layer of SHGs resulted in chaotic mixing (Figure 5f). When the second layer of SHGs was added to the top of the channel the mixing of the two streams of dye solution was nearly completed after the second mixing cycle (Figure 5g). Detailed characterization of the process of mixing using such structures can be referred in refs. [46,47].

We note that fabrication of micromixer consisting of SHGs at one surface can be achieved in photolithography with multiple steps and alignment.^[11,48] Alternatively, an SHGs mixer placed on the top and bottom of a channel can be achieved by using a milling machine and fabricate parts separately before assembling them together. However due to the limited resolution conferred by milling machines, achieved dimensions were above microscale.^[11] Sacrificial molding combined with additive manufacturing, provided simple route to fabricate channels with such complex topologies inside the channel.

3. Conclusion

In this paper, we presented a method by sacrificial molding to fabricate microchannels in various polymer matrices. The method used FDM 3D printer and PVA filaments, both of which were commercially available. The 3D printed PVA molds can be embedded in heat and photocurable polymer matrices, and PVA molds were readily dissolved in water to reveal the microchannels in desired matrices. Using the method we developed, we demonstrated fabrication of 3D microchannels—channels that have in-channel features as well as 3D networks of microchannels. We have also demonstrated a modular assembly of 3D printed molds to create multilayer networks of microchannels. Our method offers three complementary advantages to softlithography and direct 3D printing to fabricate microchannels. First, the entire process to fabricate microchannels can be performed in aqueous conditions. This method shall be readily extended to the fabrication of microchannels in cell-laden matrices. Second, the method is compatible with both heat and photocurable polymer matrices. As it stands, SLA 3D printing is limited by the availability of specific photocurable materials to fabricate the structures. Our method provided a route for the fabrication of microchannels using materials that would not be easily compatible with replica molding and 3D printing. Finally, the entire fabrication can be performed using commercially available, low-cost materials and instruments. Channels and in-channel features can be easily designed by CAD software, and patterned by a 3D printer. The simplicity and versatility of this fabrication method should be adapted by researchers without extensive background in microfabrication and microfluidics.

Resolution of 3D printed molds, which would determine the resolution of microchannels, can be optimized further. In this work, we have demonstrated the resolution of printing in the multiples of 200 μm in the horizontal dimension (x and y) and in the multiples of 100 μm in the vertical dimension (z). These resolutions are determined by the specification of the 3D printer to be used for fabricating molds. Specifically, the horizontal dimension is determined by the diameter of nozzle to extrude filaments, and the vertical dimension is determined by the layer height determined by the movement of the printing

bed. Improvements of the resolution by sacrificial molding are currently investigated in our laboratory.

A key benefit of sacrificial molding of water-soluble substrates is the capability of fabricating microfluidic channels with complex networks arranged in 3D structures in biocompatible materials (i.e., hydrogels). Recently, 3D arrangement of microfluidic channels was used to recapitulate biological systems on chip.^[20,21] In particular, 3D microfluidic channels together with appropriate biocompatible materials mimic in vivo microenvironment by the introduction of hydrodynamics,^[49] locomotion,^[50] and other critical cues for the functions of cells and living systems. We believe our work contribute to these fields by providing a simple and affordable route to fabricate complex microfluidic systems in biocompatible matrices.

4. Experimental Section

Design and Fabrication of PVA Mold: PVA molds were designed using commercially available 3D CAD software (AutoCAD 2015, Autodesk, Inc., San Rafael, CA, USA). CAD designs were exported to a standard triangulation language file format, which is then sliced into individual layers by CreatorK software (ROKIT, Seoul, South Korea) to form G-codes. G-codes are then interpreted by the ROKIT 3dison multiprinter (ROKIT, Seoul, South Korea) to fabricate a mold in a layer-by-layer manner. The bed of the printer was leveled by manually adjusting the screws at four corners of the print bed. A paper with the thickness of 100 μm was used as a spacer between the nozzle outlet and the bed to calibrate first layer height of 100 μm . PVA filament (ROKIT, Seoul, South Korea) was trimmed into strips of ≈ 100 cm and baked overnight in a 60 $^{\circ}\text{C}$ oven before printing. The diameter of the extruder was 200 μm , and the temperature of nozzle was 190 $^{\circ}\text{C}$. The object infill parameter was set to 100% to obtain solid print and layer height was set at 100 μm .

Fabrication of Microchannels in Various Matrices: PDMS prepolymer and the curing agent (Sylgard 184, Dow Corning, Midland, MI, USA) were prepared in a ratio of 10:1 by weight. A thin base layer was casted and cured prior to embedding any PVA mold. PDMS was then poured slowly onto the mold with a short segment of PTFE tube (Weico Wire and Cable Inc, Edgewood, NY, USA) attached. The PDMS and embedded mold was degassed under vacuum for 30 min, and then allowed to cure at 60 $^{\circ}\text{C}$ for 2 h. Rigid polyurethane (Crystal Clear 200, Smooth-on, Macungie, PA, USA) was prepared in a ratio of 100: 90 (Part A: Part B, as provided by the manufacturer) by weight. Flexible polyurethane (Clear Flex 30, Smooth-on, Macungie, PA, USA) was prepared in a ratio of 100: 94 (Part A: Part B, as provided by the manufacturer) by weight. Epoxy (EpoxAcast 690, Smooth-on, Macungie, PA, USA) was prepared in a ratio of 100: 30 (Part A: Part B, as provided by the manufacturer) by weight. Both polyurethanes and epoxy were handled in a chemical fume hood. The mixture was manually mixed in less than 1 min and degassed under vacuum to remove any trapped air bubbles for 10 min. Thereafter, a thin layer of polymer was slowly poured onto the PDMS coated dish and left to cure on a 65 $^{\circ}\text{C}$ hotplate for 1 h 30 min. The PVA mold attached with PTFE tubes was then placed on top of the polymer layer. At this point of time, the polymer layer was tacky, or only partially cured. Freshly degassed mixture of uncured polymer was then poured to embed the mold and tubes and degassed for 15 min. The degassed polymer with PVA mold was then placed onto the 65 $^{\circ}\text{C}$ hotplate for 30 min before curing at 60 $^{\circ}\text{C}$ for 2 h. NOA 81 (Norland Products Inc., Cranbury, NJ, USA) was used as purchased. A thin layer of NOA 81 was dispensed slowly onto the PDMS coated dish and exposed to UV in a UV flood box (UVR 600, Technodigm Innovation, Singapore) for 10 s and at 100% intensity. Fresh NOA 81 was dispensed from the bottle to embed the PVA mold attached with PTFE tubes. The NOA 81 resin and the embedded mold was then transferred carefully into the UV flood box and exposed to UV light for 15 s and at 100% intensity. PEGDA-700

(poly(ethylene glycol) diacrylate) (20% v/v) (Sigma-Aldrich, Singapore) was prepared in deionized water. Irgacure 1173 initiator (2-hydroxy-2-methylpropiophenone-97%) (0.5% v/v) (Sigma-Aldrich, Singapore) was added into the PEDGA solutions to form a prepolymer mixture. The mixture was protected from light and stored at 4 °C until it is ready to use. A thin layer of the prepolymer mixture was dispensed by a dropper onto a noncoated petri dish. A thin layer of the prepolymer mixture was then exposed to UV for 5 s and at 100% intensity. Thereafter, a fresh prepolymer mixture was used to embed the mold attached with the PTFE tubes. The prepolymer mixture and the mold were then carefully transferred to the UV flood box and exposed to UV light for additional 5 s and at 100% intensity. Transglutaminase crosslinked gelatin (TG gelatin) was prepared by first creating a 15% wt/v gelatin (gelatin from porcine skin gel strength 300, Type A (Sigma-Aldrich, Singapore) solution in sterilized Dulbecco's Phosphate-Buffered Saline (D-PBS) solution). The solution was heated in a water bath at 60 °C under magnetic stirring until the solution turned clear. The transglutaminase (Moo Gloo, Modernist Pantry, Eliot, ME, USA) was prepared at 10% wt/v in sterile D-PBS (–) solution without Ca and Mg (Nacalai Tesque, Kyoto, Japan). The solution was filtered with a 0.2 µm hydrophilic filter (Minisart, Sartorius Stedim Biotech, Göttingen, Germany) under sterile condition. The transglutaminase solution was mixed using a magnetic stirrer until the solution turned clear. Thereafter, the transglutaminase solution was added to the gelatin solution at a ratio of 1:5 under constant stirring to produce transglutaminase gelatin (TG gelatin). The TG gelatin was cooled to room temperature before use. A first layer of TG gelatin was made on an untreated petri dish on an ice bath; the solution gelled within 10 s. Thereafter, a fresh solution of TG gelatin, cooled to room temperature, was dispensed slowly to embed the PVA mold attached with PTFE tubes on an ice bath.

Removal of Mold from PDMS, PU, Epoxy and, NOA 81: After polymer resins cured, the entire polymer matrices with the embedded mold were immersed in an ultrasonic water bath (Symphony Ultrasonic bath, VWR, Padnor, PA, USA) to dissolve the embedded PVA mold in deionized water at room temperature. The removal of the sacrificial molds (T-junction, 200 µm width, 200 µm height, and 1.5 mm length) was completed in 3 h.

PEGDA: After the entire PEGDA cured, deionized water was dispensed to soak the PEGDA in a petri dish. PVA mold absorbed the water and swelled. After 1 h, the entire petri dish was gently rocked to remove the PVA mold. The process took roughly 10 min to complete.

TG Gelatin: After the entire slab of the TG gelatin solidified, sterile D-PBS solution was dispensed to soak the TG gelatin and embedded mold. The entire dish was then placed at 4 °C overnight to allow PVA mold to swell and dissolve in D-PBS solution. Fresh D-PBS solution was used to flush the microchannels for 5 min to evacuate any remaining parts of the mold. Thereafter, the TG gelatin with microchannel was sterilized in an autoclave instrument ran on a liquid cycle for 20 min at 120 °C. The device was ready for use after the autoclave treatment.

Characterization Experiments: Optical microscopy was performed on a 5.1 Megapixel Aptina digital color microscope (MU500, Amscope, Irvine, CA, USA). The microscope was calibrated using a standard ruler provided by the manufacturer. Cross-section of the PDMS channels after removal of the mold was evaluated by taking measurements at the longest dimension of width (horizontal dimension) and height (vertical dimension). Data were analyzed in Microsoft Excel (Microsoft Corporation, Seattle, Washington) and presented as mean ± SD.

The mixing experiment was analyzed by analyzing Red, Green, Blue (RGB) profile across a 1 mm line drawn across the channel (top-down view) using an RGB profile plot plugin in Image J (ImageJ, National Institutes of Health (NIH), Bethesda, MD, USA).^[51] Data were exported to Microsoft Excel to produce graphical interpretation of mixing profile. Optical images of fabricated device were taken using a Coolpix digital camera (Nikon, Tokyo, Japan). HUVECs seeded on PDMS device were visualized by fluorescence microscope (CKX53, Olympus, Tokyo, Japan).

Perfusion of Fluids: All fluids were dispensed via a syringe that was connected to sterile needles (Terumo, Tokyo, Japan) and PTFE tubing (Weico Wire and Cable, Inc, Edgewood, NY, USA). Syringe pumps (NE-4000, New Era Syringe Pump, Inc, Farmingdale, NY, USA) were used to

dispense solution from the syringe. All colored dye solutions were prepared at 20% (v/v) by mixing red, green, or blue dye (Star Brand, Kuala Lumpur, Malaysia) to deionized water. For visualization of fabricated microchannels, a solution of red dye was manually perfused to fill the channel.

Droplet Generation: The continuous phase was 3% (v/v) Span 80 (Sigma-Aldrich, Singapore) in hexadecane (Sigma-Aldrich, Singapore). The flow rate of the continuous phase was 15 µL min⁻¹. The dispersed phase was a solution of blue dye (Star Brand, Kuala Lumpur, Malaysia) in deionized water. The flow rate of the dispersed phase was 5 µL min⁻¹.

Ink permeation in TG gelatin microfluidic device: A solution of red dye was manually perfused to fill the channel. The device containing a solution of a red dye was allowed to stay at 4 °C overnight to observe the permeation of the dye in the matrix.

Mixing: Solutions of red dye and green dye were infused into separate inlets using a syringe pump at the rate of 150 µL min⁻¹. The flow was allowed to stabilize for 10 min before images were captured for analysis.

Flow Culture: A PDMS microchannel was flushed with deionized water and autoclaved in a normal cycle of 20 min at 120 °C. The surface of the microchannel was cleaned with 70% ethanol (Chemtech, Singapore) for 30 min and flushed with sterile D-PBS solution. Thereafter, the microchannel was filled with sterile porcine gelatin type A (0.02% (w/v)) and incubated in the CO₂ incubator. After incubation, the microfluidic device was flushed with D-PBS solution and dried prior to seeding of cells. HUVECs (Lifeline Cell Technology, Frederick, MD, USA) were cultured in VascuLife EnGS Endothelial Medium Complete Kit (Lifeline Cell Technology, Frederick, MD, USA) on tissue culture polystyrene flasks to 80% confluence. HUVECs from passage 4 to 6 were seeded at a density of 8 × 10⁴ cells mL⁻¹. Complete medium was continuously perfused through the channel with a syringe pump at 30 µL h⁻¹, starting at 2 h after the seeding of the HUVECs. HUVECs were grown in a humidified 5% CO₂ incubator at 37 °C. At day 4 postseeding, a live/dead assay (Invitrogen, Carlsbad, CA, USA) consisting calcein-AM/ethidium homodimer was used to stain the cells within the microchannel, according to the manufacturer's protocol.

Acknowledgements

M.H. thanks for financial supports from Start-up Research Grant at Singapore University of Technology and Design (SUTD) (SRG14088), and SUTD Digital Manufacturing and Design Centre (DManD) supported by the Singapore National Research Foundation (RGDM1620503). W.H.G. thanks for the President's Graduate Fellowship awarded by the Ministry of Education (MOE), Singapore. The authors thank Yan Linxuan for performing experiments related to flow culture of HUVECs.

Conflict of Interest

The authors declare no conflict of interest.

Keywords

3D microchannels, fused deposition modeling (FDM), microfluidics, PVA mold, sacrificial molding

Received: September 28, 2017

Revised: December 2, 2017

Published online:

[1] A. K. Au, W. Lee, A. Folch, *Lab Chip* **2014**, *14*, 1294.

[2] P. Song, W. Zhang, A. Sobolevski, K. Bernard, S. Hekimi, X. Liu, *Biomed. Microdevices* **2015**, *17*, 38.

- [3] W.-I. Wu, K. N. Sask, J. L. Brash, P. R. Selvaganapathy, *Lab Chip* **2012**, 12, 960.
- [4] Q. Xu, M. Hashimoto, T. T. Dang, T. Hoare, D. S. Kohane, G. M. Whitesides, R. Langer, D. G. Anderson, *Small* **2009**, 5, 1575.
- [5] S. Choi, M. Goryll, L. Y. M. Sin, P. K. Wong, J. Chae, *Microfluid. Nanofluid.* **2011**, 10, 231.
- [6] P. J. Kitson, M. H. Rosnes, V. Sans, V. Dragone, L. Cronin, *Lab Chip* **2012**, 12, 3267.
- [7] S. N. Bhatia, D. E. Ingber, *Nat. Biotechnol.* **2014**, 32, 760.
- [8] J. C. McDonald, D. C. Duffy, J. R. Anderson, D. T. Chiu, H. Wu, O. J. A. Schueller, G. M. Whitesides, *Electrophoresis* **2000**, 21, 27.
- [9] A. del Campo, C. Greiner, *J. Micromech. Microeng.* **2007**, 17, R81.
- [10] T. Naito, M. Nakamura, N. Kaji, T. Kubo, Y. Baba, K. Otsuka, *Micromachines* **2016**, 7, 82.
- [11] P. B. Howell Jr., D. R. Mott, S. Fertig, C. R. Kaplan, J. P. Golden, E. S. Oran, F. S. Ligler, *Lab Chip* **2005**, 5, 524.
- [12] S. Mllenbeck, N. Bogdanski, M. Wissen, H.-C. Scheer, J. Zajadacz, K. Zimmer, *Microelectron. Eng.* **2007**, 84, 1007.
- [13] Y. Hwang, R. N. Candler, *Lab Chip* **2017**, 17, 3948.
- [14] V. Gupta, M. Talebi, J. Deverell, S. Sandron, P. N. Nesterenko, B. Heery, F. Thompson, S. Beirne, G. G. Wallace, B. Paull, *Anal. Chim. Acta* **2016**, 910, 84.
- [15] S. Lee, H. Kim, D.-J. Won, J. Lee, J. Kim, *Microfluid. Nanofluid.* **2016**, 20, 1.
- [16] M. D. Symes, P. J. Kitson, J. Yan, C. J. Richmond, G. J. T. Cooper, R. W. Bowman, T. Vilbrandt, L. Cronin, *Nat. Chem.* **2012**, 4, 349.
- [17] A. Tocchio, M. Tamplenizza, F. Martello, I. Gerges, E. Rossi, S. Argenti, S. Rodighiero, W. Zhao, P. Milani, C. Lenardi, *Biomaterials* **2015**, 45, 124.
- [18] S. Mohanty, L. B. Larsen, J. Trifol, P. Szabo, H. V. R. Burri, C. Canali, M. Dufva, J. Emnéus, A. Wolff, *Mater. Sci. Eng., C* **2015**, 55, 569.
- [19] A. P. Golden, J. Tien, *Lab Chip* **2007**, 7, 720.
- [20] J. S. Miller, K. R. Stevens, M. T. Yang, B. M. Baker, D.-H. T. Nguyen, D. M. Cohen, E. Toro, A. A. Chen, P. A. Galie, X. Yu, R. Chaturvedi, S. N. Bhatia, C. S. Chen, *Nat. Mater.* **2012**, 11, 768.
- [21] L. M. Bellan, S. P. Singh, P. W. Henderson, T. J. Porri, H. G. Craighead, J. A. Spector, *Soft Matter* **2009**, 5, 1354.
- [22] L. E. Bertassoni, M. Cecconi, V. Manoharan, M. Nikkhah, J. Hjortnaes, A. L. Cristino, G. Barabaschi, D. Demarchi, M. R. Dokmeci, Y. Yang, A. Khademhosseini, *Lab Chip* **2014**, 14, 2202.
- [23] D. B. Kolesky, K. A. Homan, M. A. Skylar-Scott, J. A. Lewis, *Proc. Natl. Acad. Sci. USA* **2016**, 113, 3179.
- [24] L. M. Bellan, M. Pearsall, D. M. Cropek, R. Langer, *Adv. Mater.* **2012**, 24, 5187.
- [25] J. B. Lee, X. Wang, S. Faley, B. Baer, D. A. Balikov, H.-J. Sung, L. M. Bellan, *Adv. Healthcare Mater.* **2016**, 5, 781.
- [26] D. Theriault, S. R. White, J. A. Lewis, *Nat. Mater.* **2003**, 2, 265.
- [27] D. P. Parekh, C. Ladd, L. Panich, K. Moussa, M. D. Dickey, *Lab Chip* **2016**, 16, 1812.
- [28] V. Saggiomo, A. H. Velders, *Adv. Sci.* **2015**, 2, 1500125.
- [29] M. K. Gelber, R. Bhargava, *Lab Chip* **2015**, 15, 1736.
- [30] D. T. Pham, R. S. Gault, *Int. J. Mach. Tools Manuf.* **1998**, 38, 1257.
- [31] S. Li, Y.-Y. Liu, L.-J. Liu, Q.-X. Hu, *ACS Appl. Mater. Interfaces* **2016**, 8, 25096.
- [32] T. J. Mason, E. D. Cordemans, *Chem. Eng. Res. Des.* **1996**, 74, 511.
- [33] B. Ibarlucea, C. Fernández-Sánchez, S. Demming, S. Büttgenbach, A. Llobera, *Analyst* **2011**, 136, 3496.
- [34] M. Hashimoto, R. Langer, D. S. Kohane, *Lab Chip* **2013**, 13, 252.
- [35] K. Domansky, D. C. Leslie, J. McKinney, J. P. Fraser, J. D. Sliz, T. Hamkins-Indik, G. A. Hamilton, A. Bahinski, D. E. Ingber, *Lab Chip* **2013**, 13, 3956.
- [36] J. M. Martel, M. Toner, *Sci. Rep.* **2013**, 3, 3340.
- [37] E. J. Lim, T. J. Ober, J. F. Edd, S. P. Desai, D. Neal, K. W. Bong, P. S. Doyle, G. H. McKinley, M. Toner, *Nat. Commun.* **2014**, 5, 4120.
- [38] Z. T. Cygan, J. T. Cabral, K. L. Beers, E. J. Amis, *Langmuir* **2005**, 21, 3629.
- [39] P. Wglij, A. Homsy, N. F. de Rooij, *Sens. Actuators, B* **2011**, 156, 994.
- [40] L.-H. Hung, R. Lin, A. P. Lee, *Lab Chip* **2008**, 8, 983.
- [41] J. J. Moon, M. S. Hahn, I. Kim, B. A. Nsiah, J. L. West, *Tissue Eng., Part A* **2009**, 15, 579.
- [42] A. Paguirigan, D. J. Beebe, *Lab Chip* **2006**, 6, 407.
- [43] A. Ito, A. Mase, Y. Takizawa, M. Shinkai, H. Honda, K.-I. Hata, M. Ueda, T. Kobayashi, *J. Biosci. Bioeng.* **2003**, 95, 196.
- [44] A. P. McGuigan, M. V. Sefton, *Proc. Natl. Acad. Sci. USA* **2006**, 103, 11461.
- [45] J. S. Chohan, R. Singh, *Rapid Prototyping J.* **2017**, 23, 495.
- [46] A. D. Stroock, *Science* **2002**, 295, 647.
- [47] S. Hossain, A. Husain, K. Y. Kim, *Eng. Appl. Comput. Fluid Mech.* **2011**, 5, 506.
- [48] E. Tth, E. Holczer, K. Iván, P. Fürjes, *Micromachines* **2014**, 6, 136.
- [49] C. Buchanan, M. N. Rylander, *Biotechnol. Bioeng.* **2013**, 110, 2063.
- [50] G. M. Price, K. H. K. Wong, J. G. Truslow, A. D. Leung, C. Acharya, J. Tien, *Biomaterials* **2010**, 31, 6182.
- [51] C. A. Schneider, W. S. Rasband, K. W. Eliceiri, *Nat. Methods* **2012**, 9, 671.